

Tetracritical Behavior of CsMnBr₃

B. D. Gaulin, T. E. Mason, and M. F. Collins

Department of Physics, McMaster University, Hamilton, Ontario, Canada L8S 4M1

J. Z. Larese

Chemistry Department, Brookhaven National Laboratory, Upton, New York 11973

(Received 1 December 1988)

We have used elastic neutron scattering to determine the magnetic phase diagram of CsMnBr₃, an *XY* antiferromagnet on a stacked triangular lattice. The application of a field along (100) splits the antiferromagnetic transition and results in an intermediate phase of spin-flop character. This phase is extremely narrow near the zero-field transition at $T_N=8.32$ K which is shown to be a tetracritical point. This suggests that the unusual critical properties of the zero-field phase transition may be due to its tetracriticality as opposed to belonging to a new universality class.

PACS numbers: 64.60.Kw, 75.25.+z, 75.30.Kz, 75.40.Cx

Over the years there has been considerable interest, both experimentally and theoretically, in phase diagrams exhibiting multicritical points. Bicritical points associated with a first-order spin-flop transition have been observed in uniaxial antiferromagnets such as MnF₂.¹ Tricritical points have been studied in systems including ³He-⁴He mixtures² and the metamagnet FeCl₂.³ Mean-field and renormalization-group calculations predicted that *XY* antiferromagnets in tetragonal lattices would have a tetracritical point at $T=T_N$, $H=0$.⁴ Neutron-scattering studies of the magnetic phase diagram of Fe₂As failed to reveal the expected tricritical behavior.⁵ This discrepancy was attributed to the presence of local uniaxial strain. Tetracritical behavior has been observed in stressed LaAlO₃⁶ and GdAlO₃ in an applied magnetic field.⁷ Recently, Landau-type mean-field theory has been used to study the magnetic phase diagrams of uniaxial and planar antiferromagnets in hexagonal crystals.⁸ For the planar (*XY*) case, a tetracritical point is predicted for $T=T_N$, $H=0$; novel multicritical points may also occur at nonzero fields depending on the exact nature of the anisotropies in the system.

CsMnBr₃ has a hexagonal lattice structure, space group $P6_3/mmc$, with $a=7.61$ Å and $c=6.52$ Å at room temperature.⁹ The magnetic lattice is simple hexagonal with Mn⁺²-Mn⁺² separation of 3.2 Å along c and 7.6 Å in the a - b plane. The magnetic properties, in zero field, of this compound are well described by the Hamiltonian

$$= 2J_c \sum_i \mathbf{S}_i \cdot \mathbf{S}_{i+\Delta_c} + 2J_{ab} \sum_i \mathbf{S}_i \cdot \mathbf{S}_{i+\Delta_{ab}} + D \sum_i (S_i^z)^2,$$

with $J_c=0.88$ meV, $J_{ab}=0.0019$ meV, and $D=0.014$ meV.¹⁰ The anisotropy of the antiferromagnetic interactions ($J_c/J_{ab} \sim 460$) leads to quasi-one-dimensional behavior above 10 K.¹¹ The *XY*-like anisotropy D restricts the spins to the a - b plane below about 20 K.

In zero field, CsMnBr₃ orders three dimensionally at $T_N=8.32$ K.¹² This transition has unusual criteria exponents associated¹³⁻¹⁶ with it. It has been suggested

that the transition belongs to a new universality class due to the chiral degeneracy present in the triangularly ordered phase.¹⁷ This critical point ($T=T_N$, $H=0$) is expected to be a tetracritical point since CsMnBr₃ falls into the category covered by Ref. 8. Previous measurements have shown that the application of a 3.7-T field along (100) splits the zero-field transition.¹⁰ The nature of the intermediate phase and the phase diagram in a field were not determined. Zero-temperature classical calculations¹⁸ taking into account quantum renormalization of the spin- $\frac{5}{2}$ moment have predicted a transition from the six-sublattice triangular structure to a four-sublattice structure at $H_c=6.1$ T ($T=0$ K).

We have used measurements of the elastic neutron scattering from CsMnBr₃ to determine the nature of the intermediate phase for $H \neq 0$ and to map out the magnetic phase diagram. The measurements were carried out on the H5 triple-axis spectrometer at the Brookhaven National Laboratory high-flux beam reactor. The spectrometer was operated in elastic mode using the (002) reflection from pyrolytic graphite to monochromatize and analyze the neutron energy. All measurements were made using an incident neutron energy of 13.8 meV; a pyrolytic graphite filter was placed in the main beam in order to remove higher-order contamination. Collimation before and after the sample was 20'. The temperature was monitored by a carbon-glass resistor. The sample was mounted in an aluminum sample can filled with helium exchange gas to insure good thermal contact. Temperature stability was better than 20 mK for 7 K $< T < 10$ K, and below 7 K it was better than 10 mK. Magnetic fields between 0 and 6.5 T were applied along (100) using a split-coil superconducting magnet mounted in a vertical configuration. The crystal was mounted in the (hhl) scattering plane and is the same sample used for zero-field critical-exponent measurements.¹³⁻¹⁵

Figure 1 shows the intensity of the $(\frac{1}{3}, \frac{1}{3}, 1)$ and $(\frac{2}{3}, \frac{2}{3}, 1)$ magnetic Bragg peaks as a function of temper-

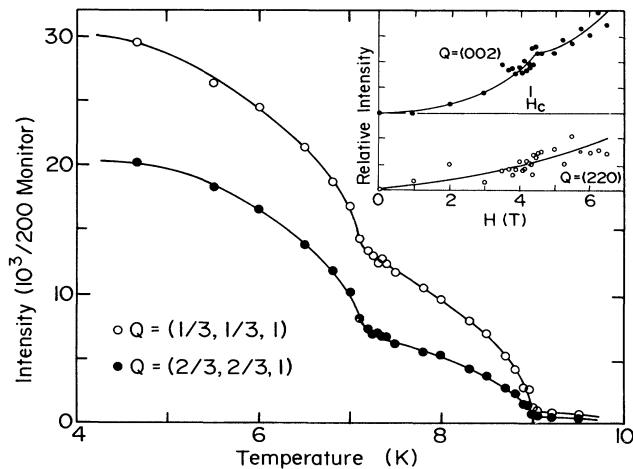


FIG. 1. The temperature dependence of the $(\frac{1}{3}, \frac{1}{3}, 1)$ and $(\frac{2}{3}, \frac{2}{3}, 1)$ magnetic Bragg intensities in a magnetic field of 4.2 T applied in the (100) direction. Successive phase transitions from the paramagnetic phase to the spin-flopped phase and from the spin-flop to the triangular phase occur at $T_{II}=9.00 \pm 0.10$ K and $T_I=7.15 \pm 0.10$ K, respectively. Inset: Field dependence of the intensity of the (220) and (002) Bragg peaks for $T=7.0$ K, indicating the increasing component of the moment parallel to the field.

ature in an applied field of 4.2 T. Two phase transitions are evident in the data, one from the paramagnetic to a long-range ordered state at $T_{II}=9.00 \pm 0.10$ K and a second between two ordered phases at $T_I=7.15 \pm 0.10$ K. The inset shows the field dependence of the intensities of the (220) and (002) reflections at $T=7.0$ K relative to the zero-field nuclear intensity. There is a gradual increase with field due to the increasing component of the moment parallel to the field. There is some evidence for a kink in the (002) data although the statistics are rather poor due to the large nuclear component of the intensity.

We have performed similar temperature scans at various field values and, at lower temperatures, field scans at constant temperature in order to map out the phase diagram of CsMnBr_3 in an applied field. The results are shown in Fig. 2. The intensities of the magnetic peaks observed in both phases $[(\frac{1}{3}, \frac{1}{3}, 1)$, $(\frac{2}{3}, \frac{2}{3}, 1)$, $(\frac{4}{3}, \frac{4}{3}, 1)$ and $(\frac{1}{3}, \frac{1}{3}, 3)]$, along with the field dependence of the ferromagnetic component (inset, Fig. 1), are consistent with the zero-temperature predictions for the two phases.¹⁸ The low-field, low-temperature phase (I) is the triangular phase with an increasing cant toward the field direction and an increasing component perpendicular to the field that alternates antiferromagnetically from layer to layer. At the transition from phase I to phase II, the six sublattices collapse to four and the spins continue to cant toward the field and the perpendicular component decreases upon increasing the field. These magnetic structures are shown schematically in Fig. 2 for both

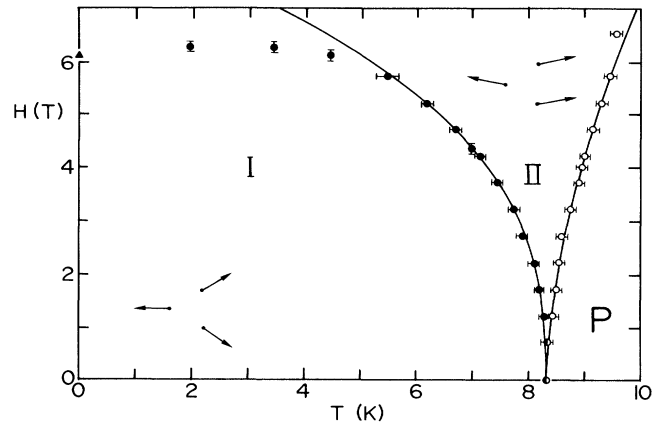


FIG. 2. The phase diagram of CsMnBr_3 in a magnetic field applied along (100). P denotes the paramagnetic phase, II the spin-flop phase, and I the triangular phase. Representative spin configurations (see text) for a triad of nearest-neighbor spins within the basal plane in each of the ordered phases are shown on the phase diagram. The lines are the results of least-squares fits by power laws near the tetracritical point described in the text.

phases. The structures shown are for a field applied along the positive y axis of the graph and the spin configurations represent those taken up by a triad of nearest-neighbor spins within the basal plane.

All the data suggest that both phase boundaries are continuous over the measured range. Temperature scans were carried out by increasing and decreasing the temperatures, and no hysteresis was observed. The lines in the phase diagram correspond to the least-squares fits of the critical temperatures at finite field by the power-law behavior that is predicted⁴ to hold near the tetracritical point appropriate to the tetragonal XY -like antiferromagnets:

$$\frac{T_i(H^2) - T_N}{T_N} \propto (H^2)^{1/\psi_i}$$

We find $\psi_{P-II}=1.21 \pm 0.07$ and $\psi_{II-I}=0.75 \pm 0.05$, where the ψ_i 's are crossover exponents appropriate to the phase boundaries. The second of these exponents does not agree with the prediction,⁴ a result which may be expected because of the different physical origins of the tetracriticality. In the case of CsMnBr_3 , the tetracriticality is due to the symmetry of the lattice, while for the tetragonal XY -like antiferromagnets, the tetracriticality arises due to anisotropic terms in the Hamiltonian. The fact that both exponents are less than 2 means both phase boundaries cross the $H=0$ T line at 90° . This reflects the fact that the intermediate spin-flop phase (II) is extremely narrow near the tetracritical point. The nature of the phase diagram around the tetracritical point is qualitatively quite different from previously observed cases^{6,7}; it more closely resembles the behavior predicted⁴ but not observed⁵ for Fe_2As . The triangle

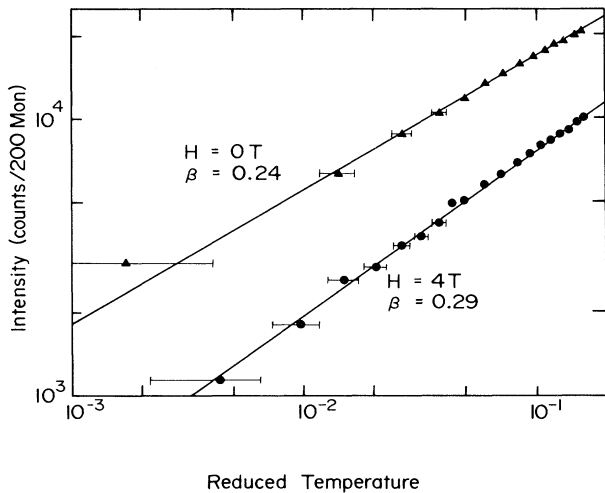


FIG. 3. Log-log plot of the $(\frac{1}{3}, \frac{1}{3}, 1)$ magnetic Bragg peak intensity (\propto square of the sublattice magnetization) vs the reduced temperature for the spin-flop phase ($H=4.0$ T) and the tetracritical point ($H=0.0$ T). The lines are the results of least-squares fits by power laws with the critical exponents β as indicated.

plotted on the $T=0$ K line of Fig. 2 corresponds to the predicted zero-temperature transition field of 6.1 T.¹⁸ Extrapolating the measured transition field results in an estimated zero-temperature transition field of 6.2 ± 0.5 T.

The measured magnetic Bragg peak intensity is proportional to the square of the sublattice magnetization. We have used the measured intensities to determine the critical exponent β for $H=4.0$ T which we find to be 0.29 ± 0.02 . This value is consistent with the 3D Ising order parameter expected for the spin-flop phase. The zero-field value was found to be $\beta=0.24 \pm 0.02$ consistent with previously determined values^{13,16} and the theoretical predictions.¹⁷

The application of the magnetic field within the basal plane is expected to have a pronounced effect on the critical properties of the material. First, it breaks the XY -like symmetry within the basal plane. Second, the spin-flop phase does not possess the chiral degeneracy present in the triangular antiferromagnetic phase. Consequently, three-dimensional Ising-type critical behavior is expected on physical grounds for the paramagnetic to spin-flop phase transition.

The data and the results of the least-squares fits by power laws in reduced temperature for the $(\frac{1}{3}, \frac{1}{3}, 1)$ peak are shown in Fig. 3. The values of β were determined using data from the $(\frac{1}{3}, \frac{1}{3}, 1)$ and $(\frac{2}{3}, \frac{2}{3}, 1)$ magnetic Bragg peaks and no systematic differences were observed for the two peaks. The previous determination of β in zero field¹³ made use of the $(\frac{1}{3}, \frac{1}{3}, 1)$, $(\frac{4}{3}, \frac{4}{3}, 1)$, and $(\frac{1}{3}, \frac{1}{3}, 3)$ peaks and no systematic differences due to

extinction were observed in that case, so we do not believe extinction is a significant source of error for this crystal.

It has been suggested that the zero-field transition of CsMnBr_3 belongs to a new universality class characterized by the symmetry of the order parameter, $Z_2 \times S_1$.¹⁷ This differs from the standard XY model (S_1) due to the presence of a chiral degeneracy (Z_2) in the triangular phase. The present work permits an alternate explanation for the unusual critical exponents¹³⁻¹⁶ observed in this system. The fact that the transition at $T=T_N=8.32$ K, $H=0$ is a tetracritical point is perhaps sufficient to explain the anomalous critical exponents without the need for extending the concept of universality to include the symmetry of the order parameter instead of just its dimensionality.

We would like to thank Dr. A. Caille, Dr. A. J. Berlinsky, Dr. C. Kallin, Dr. M. L. Plumer, and Dr. S. M. Shapiro for helpful discussions. Two of us (B.D.G. and T.E.M.) gratefully acknowledge the hospitality of Brookhaven National Laboratory. Research at McMaster University was supported by the Natural Sciences and Engineering Research Council of Canada and by the Ontario Centre for Materials Research. Research at Brookhaven National Laboratory was supported by the Division of Materials Science, U.S. Department of Energy under Contract No. DE-AC02-76CH00016.

¹Y. Shapira and S. Foner, Phys. Rev. B **1**, 3083 (1970).

²E. H. Graf, D. M. Lee, and J. D. Reppy, Phys. Rev. Lett. **19**, 417 (1967).

³R. J. Birgeneau, G. Shirane, M. Blume, and W. C. Koehler, Phys. Rev. Lett. **33**, 1098 (1974).

⁴M. Kerszberg and D. Mukamel, Phys. Rev. B **18**, 6283 (1978).

⁵L. M. Corliss, J. M. Hastings, W. Kunnmann, R. J. Begum, M. F. Collins, E. Gurewitz, and D. Mukamel, Phys. Rev. B **25**, 245 (1982).

⁶K. A. Muller, W. Berlinger, J. E. Drumheller, and J. G. Bednorz, in *Multicritical Phenomena*, edited by R. Pynn and A. Skjeltorp (Plenum, New York, 1983), p. 143.

⁷H. Rohrer and Ch. Gerber, Phys. Rev. Lett. **38**, 909 (1977).

⁸M. L. Plumer, A. Caille, and K. Hood, Phys. Rev. B **39**, 4489 (1989).

⁹J. Goodyear and D. J. Kennedy, Acta Crystallogr. Sect. B **28**, 1640 (1974).

¹⁰B. D. Gaulin, M. F. Collins, and W. J. L. Buyers, J. Appl. Phys. **61**, 3409 (1987).

¹¹B. D. Gaulin, M. F. Collins, Can. J. Phys. **62**, 1132 (1984).

¹²M. Eibshutz, R. C. Sherwood, H. S. L. Fsu, and D. E. Cox, in *Thermal Expansion—1973*, edited by R. E. Taylor and G. L. Denman, AIP Conference Proceedings No. 17 (American Institute of Physics, New York, 1974).

¹³T. E. Mason, B. D. Gaulin, and M. F. Collins, *J. Phys. C* **20**, L945 (1987).

¹⁴B. D. Gaulin, M. F. Collins, and T. E. Mason, *Physica (Amsterdam) B* (to be published).

¹⁵T. E. Mason, B. D. Gaulin, and M. F. Collins, *Phys. Rev. B* **39**, 586 (1989).

¹⁶Y. Ajiro, T. Nakashima, Y. Unno, H. Kadowaki, M. Mekata, and N. Achiwa, *J. Phys. Soc. Jpn.* **57**, 2648 (1988); H. Kadowaki, S. M. Shapiro, T. Inami, Y. Ajiro, *J. Phys. Soc. Jpn.* **57**, 2640 (1988).

¹⁷H. Kawamura, *J. Appl. Phys.* **63**, 3086 (1988).

¹⁸A. V. Chubukov, *J. Phys. C* **21**, L441 (1988).